Mechanistic Effects of Autophosphorylation on Receptor Tyrosine Kinase Catalysis: Enzymatic Characterization of Tie2 and Phospho-Tie2

Brion W. Murray,* Ellen S. Padrique, Chris Pinko, and Michele A. McTigue

Pfizer Global Research and Development La Jolla Laboratories, 4215 Sorrento Valley Boulevard, La Jolla, California 92121

Received May 10, 2001; Revised Manuscript Received June 19, 2001

ABSTRACT: Activation of receptor tyrosine kinases by autophosphorylation is one of the most common and critical transformations in signal transduction, yet its role in catalysis remains controversial. Autophosphorylation of the angiogenic receptor tyrosine kinase Tie2 was studied in terms of the autophosphorylation sites, sequence of phosphorylation at these sites, kinetic effects, and mechanistic consequences. Isoelectric focusing electrophoresis and mass spectrometric analysis of a Tie2 autophosphorylation time course showed that Tyr992 on the putative activation loop was phosphorylated first followed by Tyr1108 in the C-terminal tail (previously unidentified autophosphorylation site). Autophosphorylation of Tie2 to produce pTie2 resulted in a 100-fold increase in k_{cat} and a 460-fold increase in k_{cat}/K_m. Viscosity studies showed that the unphosphorylated Tie2 was partially limited by product diffusion ($(k_{cat})^{\eta} = 0.67 \pm 0.06$), while product release was more rate-limiting ($(k_{cat})^{\eta} = 0.94 \pm 0.08$) for autophosphorylated Tie2 (pTie2). Furthermore, autophosphorylation did not significantly affect the phosphoacceptor dissociation constants. There was a significant $(k_{cat})^{H}/(k_{cat})^{D}$ solvent isotope effect (SIE) for unphosphorylated Tie2 (2.42 ± 0.12) and modest SIE (1.28 ± 0.04) for pTie2, which is consistent with the chemistry step being more rate-limiting for Tie2 as compared to pTie2. The pH-rate profiles of Tie2 and pTie2 revealed a >0.5 unit shift in the pK_a values of catalytically relevant ionizable residues upon autophosphorylation. The shift in rate-limiting step will result in a different distribution of enzyme pools (e.g., E, E•S, E•P, etc.) which may modulate the susceptibility to inhibition. Tie2 and pTie2 were profiled with a panel of known ATP-competitive kinase inhibitors. Tie2 activation perturbs catalytic residue ionizations, shifts the rate-limiting step to almost exclusive diffusion-control, and transforms the kinase into a more perfect catalyst.

Autophosphorylation of receptor tyrosine kinases is a central mechanism for signal transduction. Receptor tyrosine activation is generally believed to be due to ligand-induced receptor dimerization: the extracellular receptor domain dimerization brings the cytosolic kinase domains vicinal for intermolecular autophosphorylation (*1*, *2*). Autophosphorylation has multiple functions including enhancement of the kinase activity and production of sites in the C-terminal tail for recruitment of downstream signaling molecules. Kinase activation usually occurs by autophosphorylation of a residue(s) in an activation loop (A-loop) in subdomain VIII of the C-terminal lobe (*3*). Structural studies of receptor tyrosine kinases have shown that autophosphorylation effects global changes in the structure including a rotation of the N-terminal lobe toward the C-terminal lobe (*4*, *5*). Autophosphorylation also has a substantial impact on receptor tyrosine kinase biology.

Signaling from Tie2[1] (tyrosine kinase with immunoglobulin and EGF homologous regions; TEK) an angiogenic receptor tyrosine kinase (RTK) expressed almost exclusively on vascular endothelial cells, results in survival of newly formed blood vessels through an anti-apoptotic response and recruitment of stabilizing interactions with smooth muscle cells (*6*−*8*). Tie2 was identified as an endothelium specific kinase through PCR-based screens for novel receptor tyrosine kinases (*9*−*14*). Studies have shown that the receptor ligand angiopoietin-1 and angiopoeitin-4 upregulates Tie2 activity (*15*) while the ligands angiopoietin-2 and angiopoietin-3 downregulate Tie2 activity (*15*−*17*). Tie2 receptor activation includes autophosphorylation as initially shown by [^{32}P]-phosphate incorporation into an immune complex with Tie2 (*14*). The activating autophosphorylation site in the catalytic domain on Tie2 can be predicted by sequence alignments (*3*) and has been tentatively assigned. A recent mass spectrometric study of Tie2 reported that autophosphorylation of Y992 in the activation loop was not possible without mutating Y897, Y1088, and S1119 (*18*). The active Tie2 kinase domain has been shown to be critical to its biological role (*19*−*22*). Dominant-negative and gene knockout studies

* To whom correspondence should be addressed: Tel: 1-858-622-6038. Fax: 1-858-678-8277. E-mail: brion.murray@agouron.com.

[1] Abbreviations: Tie2, tyrosine kinase with immunoglobulin and EGF homologous regions, TEK; pTie2, phospho-Tie2; SIE, solvent isotope effect; RTK, receptor tyrosine kinase; HEPES, *N*-[2-hydroxyethyl]piperazine-*N*′-[4-butanesulfonic acid]); MOPS, 3-[*N*-morpholino]-propanesulfonic acid), MES (2-[*N*-morpholino]ethanesulfonic acid); Bis-Tris propane, BTP; 1,3-bis[tris(hydroxymethyl)methylamino]propane); DTT, dithiothreitol; PKA, protein kinase A; ATP, adenosine-5′-triphosphate; MALDI-TOF MS, matrix-assisted laser desorption ionization time-of-flight mass spectrometry; nanoESI MS, nano-electrospray ionization mass spectrometry; $(k_{cat}/K_m)^{\eta}$, viscosity effect on k_{cat}/K_m; $(k_{cat})^{\eta}$, viscosity effect on k_{cat}; $(k_{cat})^{H}$, k_{cat} in H_2O; $(k_{cat})^{D}$ k_{cat} in D_2O; SH2, Src homology domain 2; PTB, phosphotyrosine binding domain.

10.1021/bi010959e CCC: $20.00
Published on Web 08/03/2001

have shown that Tie2 has a critical role in proliferation, differentiation, and survival of endothelial cells (*19*). Mutations that produce enhanced Tie2 autophosphorylation by a ligand-independent process have been shown to cause hereditary malformations of the vasculature (*23*, *24*). Autophosphorylation of the C-terminal tail has been shown to be critical to the recruitment of the many signaling molecules including the following: Grb2, Grb7, Grb14, Shp2, p85 subunit of PI3K, and Dok-R (*20*−*22*, *25*). To date, there have been no enzymatic studies of Tie2 reported in the literature or any studies of the kinetic effects of Tie2 activation.

Although the mechanistic consequences of autophosphorylation are poorly understood, the mechanisms of protein kinases have been studied extensively. The paradigm for mechanistic understanding of protein kinases is the serine/threonine kinase cAMP-dependent protein kinase (PKA). Through kinetic, structural, and mutational analysis of PKA, the enzyme mechanism is a sequential (ternary complex of PKA, ATP, and peptide) with an ordered or preferred order of substrate addition (*26*−*31*). Evidence that the chemical step (phosphate transfer) is not rate-limiting: PKA activity has a strong viscosity dependence $(k_{cat})^{\eta} = 0.9-1.1$ (*32*, *33*), a small D_2O solvent isotope effect ($k_{cat}H/k_{cat}D = 1.6 \pm 0.4$) (*34*). Detailed pre-steady-state kinetic studies of PKA confirmed that phosphate transfer was not rate limiting (*35*). There are two catalytically relevant ionizable residues with $pK_a = 6.2$ and 8.5 (*34*), yet the role of a catalytic base in the mechanism remains controversial (*33*). Activation of PKA occurs not by phosphorylation or autophosphorylation but by dissociation of a regulatory subunit.

More recently, tyrosine kinases have been the subject of mechanistic studies: nonreceptor tyrosine kinases C-terminal Src kinase (Csk) and v-fps. Csk has a low k_{cat} (0.67 s^{-1}) and random sequential kinetic mechanism. The chemical step is not rate-limiting as demonstrated by a small D_2O SIE ($k_{cat}H/k_{cat}D = 1.2 \pm 0.1$) and a moderate viscosity effect ($(k_{cat})^{\eta} = 0.42 \pm 0.04$) (*36*−*38*). Detailed studies of the more active v-fps ($k_{cat} = 13-14$ s^{-1}) revealed a modest SIE ($k_{cat}H/k_{cat}D = 1.6$), partially rate-limiting product release ($(k_{cat})^{\eta} = 0.51-0.74$), and one catalytically relevant ionizable residue detected in the 6.0−9.5 pH range ($pK_a = 6.7 \pm 0.07$) (*39*). Furthermore, a v-fps proton inventory profile was bowed-up which was interpreted as one proton in flight in a virtual transition state where phosphate transfer and product release are both partially rate limiting (*40*). Activation of nonreceptor tyrosine kinases is thought to be due to intrasteric phenomena (*41*).

Receptor tyrosine kinases (RTK) are type I transmembrane proteins with a ligand-binding extracellular domain, a single membrane-spanning domain, a juxtamembrane region, a catalytic domain, and a C-terminal tail. Detailed analysis of an entire RTK is problematic due to the (i) membrane association, (ii) size, and (iii) multidomain complexity. Recent studies of the receptor tyrosine kinases have demonstrated the utility and validity of studying the soluble kinase domain (*42*−*46*). The aim of the present study is to characterize how tyrosine kinase autophosphorylation affects enzymatic catalysis. This work probes the kinetic consequences of autophosphorylation by kinetically characterizing the phosphorylated and unphosphorylated states of Tie2. The phosphorylation sites and order of the autophosphorylation events on Tie2 were characterized. Detailed enzymatic analysis of Tie2 and pTie2 showed that autophosphorylation enhances kinase activity by more than 2 orders of magnitude and changes the pK_a of ionizable residues. The overall effect of autophosphorylation on Tie2 is an increase in the rate of the chemical step (phosphate transfer), which makes physical steps (e.g., product release) become more rate-limiting.

MATERIALS AND METHODS

Materials. Histone 2B was purchased from Roche Molecular Biochemicals. γ-[^{32}P]-ATP was purchased from Pharmacia-Amersham. GF/B glass fiber filterplates and Microscint-20 were purchased from Packard. The following reagents were purchased from the Sigma Chemical Company: poly(Glu_4Tyr), Ac-SQNYPVV-amide, lactate dehydrogenase, pyruvate kinase, phosphoenolpyruvate, HEPES (*N*-[2-hydroxyethyl]piperazine-*N*′-[4-butanesulfonic acid]), MOPS (3-[*N*-morpholino]propanesulfonic acid), MES (2-[*N*-morpholino]ethanesulfonic acid), bis-tris propane (BTP; 1,3-bis[tris(hydroxymethyl)methylamino]propane), NaCl, dithiothreitol, $MgCl_2$, ATP, and NADH.

Tie2 Kinase Domain Expression. The intracellular kinase domain of the human Tie2 was expressed using the baculoviral vector expression system starting from nucleotides encompassing amino acid residues 774 to 1124. The sequence was identical to that reported in GenBank (L06139). This construct also had no protein expression tag and one amino acid substitution due to the need for a start codon; R774M. The Tie2 insert was ligated into a modified pFastBac vector (Life Technologies) with Nco1 and EcoR1. (The 5′ Nco1 site was generated at the endogenous ATG at bp 4000 of the vector). The construct was transfected into Sf9 cells using the pFastBac protocol to generate a high titer viral stock. All infections were made at multiplicity-of-infection of 3 with a cell density (Sf9 or Sf21) of $1-1.5 \times 10^6$. Infected cells were harvested by centrifugation after 48 h infection and stored at −70 °C.

Tie2 Protein Purification. Cells were thawed and lysed in 25 mM Mops 7.0/20 mM NaCl/5 mM DTT/5% (v/v) glycerol by sonication. Lysates were cleared by centrifugation at 35 000 rpm for 50 min. The soluble fraction was loaded onto a 35-mL Source 30 S−Sepharose (Pharmacia) column at 4 mL/min and eluted with a 20 mM−350 mM NaCl gradient in 25 mM Mops 7.0/5 mM DTT/5% (v/v) glycerol over 800 mL. Tie2 containing fractions were pooled by SDS−PAGE and by the presence of tyrosine kinase activity. Kinase activity was measured with a commercially available photometric ELISA assay kit (Roche Molecular Biochemicals). This pool was then loaded directly over a 9-mL macroprep hydroxyapatite (BioRad) column at 1 mL/min and rinsed with 3 column volumes of 25 mM HEPES 7.5/50 mM NaCl/5 mM DTT/5% glycerol. Tie2 was eluted with a 180-mL linear gradient between this buffer and 85 mM potassium phosphate 7.5/50 mM NaCl/5 mM DTT/5% glycerol. Tie2 was pooled using both SDS−PAGE and by the presence of tyrosine kinase activity (Roche Molecular Biochemicals). The Tie2 containing pool was then diluted with 3 volumes of 5 mM DTT/5% (v/v) glycerol and loaded onto an 8-mL Source 15 S-Sepharose (Pharmacia) at 2 mL/min. The column was rinsed with 25 mM HEPES 7.5/20 mM NaCl/5 mM DTT/5% (v/v) glycerol, and bound protein was eluted with a 225-

mL linear NaCl to 25 mM Tris 8.0/225 mM NaCl/5 mM DTT/5% (v/v) glycerol. Tie2-containing fractions were pooled by SDS−PAGE and by the presence of tyrosine kinase activity (Roche Molecular Biochemicals). Purified protein was dialized into a buffer containing 50 mM HEPES 7.5/250 mM NaCl/10 mM DTT/5% glycerol/0.025% Tween-20/5 mM $MgCl_2$ and flash frozen at approximately 4 mg/mL concentration.

Enzymatic Assays. A coupled enzymatic assay format was used to measure both Tie2 and pTie2 activities. The kinase-catalyzed production of ADP from ATP that accompanies phosphate transfer to the random copolymer poly(Glu_4Tyr) was coupled to the oxidation of NADH through the activities of pyruvate kinase (PK) and lactate dehydrogenase (LDH). NADH conversion to NAD^+ was monitored by the decrease in absorbance at 340 nm ($\epsilon = 6.22\ cm^{-1}\ mM^{-1}$) using a Beckman DU650 spectrophotometer. A typical reaction solution contained 1 mM phosphoenolpyruvate, 0.24 mM NADH, 40 mM $MgCl_2$, 5 mM DTT, poly(Glu_4Tyr), ATP, 15 units/mL PK, 15 units/mL LDH in 100 mM HEPES, pH 7.5. ATP was varied from 0.5 to 2000 μM and poly(Glu_4Tyr) was varied from 0.5 to 20 mg/mL. To calculate the concentration of available tyrosine residues in poly(Glu_4Tyr), the minimum unit that contains a tyrosine (Glu_4Tyr) was calculated to have a MW of 679.66. Assays were initiated with the addition of 4 to 12 nM phosphorylated Tie2 (aa 775−1122) or 50 to 125 nM unphosphorylated Tie2.

A second assay format was used to monitor the production of the other kinase product: phospho-protein. This simple radioactive assay was used to monitor the transfer of phosphate from γ-[^{32}P]-ATP to histone 2B. The glass fiber filterplate assay format measures the capture of TCA-precipitated [^{32}P]-phosphorylated proteins on glass fiber filters in a 96-well format. The kinetic parameters for Tie2 were evaluated in the filtermate assay format and were similar to the values determined in the coupled enzymatic format. Typical assay conditions were established: 5 ng of pTie2, 0.050 mM ATP, 0.5 μCi γ-[^{32}P]-ATP, 40 mM $MgCl_2$, 1 mM DTT, 0.01% Tween-20, 100 mM HEPES, pH 7.5, 0.050 mL, RT, and 30 min. These conditions deliver a signal/noise ratio greater than 20. Histone 2B was varied from 0.2 to 15 μM and ATP was varied from 5 to 400 μM.

Tie2 Autophosphorylation. Typical autophosphorylation reactions to produce maximally active pTie2 were performed at 4 °C for 4 h with the following components: 25 μM Tie2, 100 mM HEPES (pH 7.5), 40 mM $MgCl_2$, 10 mM ATP, 2 mM DTT, and 0.01% Tween-20. At fixed time points in the autophosphorylation reaction, the extent of autophosphorylation was measured for enhancement of kinase activity (coupled enzymatic assay with 2 mM ATP, variable poly(Glu_4Tyr)) and by isoelectric focusing gel electrophoresis (IEF) analysis (5 μg/time point). To address the effect of Tie2 concentration on the autophosphorylation reaction, Tie2 concentration was varied (no reaction, 5, 10, 15, 20, 25 μM Tie2) in 4 h, 4 °C autophosphorylation reactions. The resulting phospho-Tie2 preparations were diluted to a final concentration of 28.6 nM and assayed with the coupled, enzymatic assay at saturating ATP (2 mM) and saturating poly(Glu_4Tyr) (11.4 mg/mL) in duplicate to approximate V_{max} conditions. The $K_{m,ATP}$ for the Tie2 autophosphorylation reaction (0.84 μM Tie2, 12 ATP concentrations from 0 to 2000 μM) was derived by measuring ADP production in the absence of peptide or protein substrates with the coupled, enzymatic assay at 37 °C. Finally, mass spectrometry was used to identify the sites and order of phosphate incorporation into Tie2. IEF gel slices were taken along the autophosphorylation time course for mass spectrometric analysis.

Mass Spectrometry. (a) Proteolysis Experiments. The Tie2 gel slices (unphosphorylated Tie2, intermediately phosphorylated Tie2, and exhaustively phosphorylated Tie2) were destained with MeOH and then washed with 100 mM ammonium bicarbonate in 30% acetonitrile and digested with trypsin (100 ng) in 3 mM Tris-HCl at pH 8, 37 °C for overnight. The tryptic peptides were extracted out of the gel using 50% acetonitrile/0.1% TFA, concentrated to 10 μL, and subjected to MALDI and nanoESI mass analysis.

(b) MALDI/MS Analysis. All MALDI-MS analyses were performed in a Voyager-Elite; time-of-flight mass spectrometer with delayed extraction (PerSeptive Biosystems, Inc., Framingham, MA). A volume of 1 μL of digested protein was placed directly on the MALDI analysis plate, mixed with 1 μL of matrix (α-cyano-4-hydroxy-cinnamic acid) in a saturated solution of acetonitrile/water (50:50, v/v) with 0.1% (w:w) trifluoroacetic acid (TFA) and inserted into the MALDI ionization source for analysis. Samples were irradiated with a nitrogen laser (Laser Science Inc.) operated at 337 nm. The laser beam was attenuated by a neutral density filter onto the sample target. Ions produced by laser desorption were typically energetically stabilized during a delayed extraction period of 150 ns and were then accelerated through the time-of-flight mass analyzer with a 20 kV potential. Spectra shown were typically an average of 128 laser pulses.

(c) NanoESI-MS. MS/MS analyses were performed on a triple quadrupole mass spectrometer (PE Sciex API III, Alberta, Canada) modified with a nanoESI source from Protana A/S (Denmark). The ESI voltage was set at 850 V and the orifice settings were maintained at 100 V. A curtain gas of ultrapure nitrogen was pumped into the interface at a rate of 0.6 L/min to aid evaporation of solvent droplets and to prevent particulate matter from entering the analyzer. For precursor ion scan experiment, 3 μL of digested protein was mixed with 3 μL of 25 mM ammonia solution and 3 μL of methanol (pH = 9). For the product ion scan experiment, 3 μL of digested protein was mixed with 7 μL of methanol and 0.5 μL of formic acid. A 4 μL aliquot was loaded into a palladium-coated boro-silicate glass capillary and injected into the mass spectrometer. Precursor ion scanning was used to generate spectra of its precursors (or "parent" ions) of the phosphate fragment *m*/*z* 79. Product ion scan was also used to obtain the sequence information of phosphopeptides.

(d) Microcapillary HPLC-MS/MS. The microcapillary CMS/MS experiment was performed on a system of Agilent 1100 HPLC (Agilent Technologies, Palo Alto, CA) combined with Finnigan LCQ mass spectrometer (Finnigan, San Jose, CA). A 2 μL aliquot of the digested sample was mixed with 2 μL of 5% acetic acid and loaded on a capillary column. A 45-min gradient of 0−80% solvent B (A: 2% MeCN/0.02% heptafluorobutyric acid (HFBA), B: 98% MeCN/0.02% HFBA) was used to separate the tryptic peptides. The heated desolvation capillary in LCQ was held at 180 °C, the spray voltage was set at 1.8 kV, and the capillary voltage was set at 30 V. The MS/MS spectra were acquired in dependent scan mode with a collision energy of 30%, threshold at 1 × 104. The precursor ion default charge state was set to +2,

which is used to calculate the scan range for acquiring MS/MS spectra.

Viscosity Studies. Unphosphorylated Tie2 and autophosphorylated Tie2 (pTie2) enzymatic activities were evaluated as a function of sucrose microviscogen and PEG 8000 macroviscogen. Stock solutions of sucrose (50% w/v) and PEG 8000 (7.3% w/v) were used to make dilutions. The viscosities of the dilutions were established at 24 °C in triplicate with an Oswald viscometer (*47*). Each viscosity measurement was carried out with 5 mL of viscous solution. The amount of time for the viscogen to move between markings on the Oswald viscometer was measured. Data were fit to the following equation: $\eta^{rel} = (t\%\rho\%)/(t\rho)$ where t = time for water, ρ = density of water, $t\%$ = time for viscous solution, and $\%\rho$ = density of the viscous solution. The following is the relative viscosity for the viscogens: 1.3% PEG8000, 1.30; 3.2% PEG8000, 1.81; 4.2% PEG8000, 2.18; 5.2% PEG8000, 2.58; 7% sucrose, 1.19, 8% sucrose, 1.22; 10% sucrose, 1.28; 15% sucrose, 1.50; 23% sucrose, 1.93; 30% sucrose, 2.57; 34% sucrose, 3.16.

The steady-state parameters for Tie2 in the presence of different viscogens and viscogen levels were performed at a saturating ATP concentration (2 mM) and variable poly(Glu_4,Tyr) concentrations. The coupled, enzymatic assay was used to measure kinase activity. No viscosity effect was observed on the coupling enzyme system because the coupling enzymes were used in a large excess. Doubling the concentrations of the coupling enzyme had no effect on the observed Tie2 velocities. Kinetic data were fit to the Michaelis−Menten equation to derive relative k_{cat} and k_{cat}/K_m values. The kinetic parameters were plotted versus the relative viscosity and fit to a linear equation. The determined slopes for $k_{cat}\eta$ were derived from the k_{cat} versus relative viscosity plots and $(k_{cat}/K_m)^{\eta}$ from the slopes of the k_{cat}/K_m versus relative viscosity plots.

pH-Rate Studies. The pH-stabilities of Tie2 and pTie2 were measured to ensure that there was no contribution of irreversible pH-dependent denaturation in the pH−rate studies. To assess the stability of Tie2 to different pH conditions, pH swap experiments were performed. Tie2 was incubated at room temperature in a low strength pH buffer (20 mM) and then assayed in the coupled, enzymatic (CE) assay at 200 mM HEPES, pH 7.5. In addition to the differential buffer strength, the variable pH buffer was diluted upon addition to the CE buffer (5 into 175 μL). The overall dilution of the initial buffer was 360-fold, rendering the contribution of the variable pH buffer to the final HEPES pH 7.5 assay buffer to be under 0.3%. Tie2 activity was measured using the coupled enzymatic assay with poly(Glu_4,Tyr) as the phosphoacceptor. An overlapping buffer scheme was used to avoid artifactual buffer effects: MES from 5.5 to 6.5 and bis-tris propane (BTP) from 6.5 to 9.5. Both Tie2 and pTie2 were stable to irreversible pH-dependent denaturation in the examined pH range.

After the pH stabilities of Tie2 and pTie2 had been established, the pH−rate behavior was characterized. The MES and BTP buffer scheme described in the stability studies was used except there was no buffer swap into HEPES 7.5. The simple radioactive glass fiber filterplate assay format was used to measure Tie2 activity to avoid pH effects on the coupling enzymes (PK and LDH). At a constant 0.1 mM ATP, the concentration of histone 2B was varied (0, 0.25, 0.5, 1.0, 2.0, 4.0, 6.0, 8.0 μM). The final concentration of enzyme was as follows: 15.0 nM pTie2 and 1500 nM Tie2. Kinetic data were fit to the Michaelis−Menten equation to derive relative k_{cat} and k_{cat}/K_m values. The $\log(k_{cat})$ and $\log(k_{cat}/K_m)$ were plotted versus pH. The data were fit to the equations for one basic residue (eq 1) or acid and basic residues (eq 2), where y is either k_{cat} or k_{cat}/K_m values and c is the maximum value of that parameter.

$$\log(y) = \log(c/(1 + [H^+]/K_a)) \quad (1)$$

$$\log(y) = \log(c/(1 + [H^+]/K_a + K_b/[H^+])) \quad (2)$$

Solvent Isotope Studies. The coupled enzymatic assay format was modified to study the effects of D_2O on the Tie2 and pTie2 kinetic parameters. [^{2}H]-HEPES was prepared by repeatedly solvating HEPES in D_2O and lyophilizing the solution. The coupled enzymatic assay components were prepared in D_2O except for pyruvate kinase and lactate dehydrogenase which had an insignificant contribution of H_2O to the overall reaction. Poly(Glu_4,Tyr) was varied (0, 0.0914, 0.178, 0.357, 0.718, 0.357, 0.714, 1.43, 2.86, 4.29, 5.71, 7.14, 8.57, and 11.4 mg/mL) at a saturating concentration of ATP (2 mM). The final concentrations of pTie2 and Tie2 are 14.3 and 570 nM, respectively. Sucrose, at a final concentration of 7.3%, was used as viscosity control to compensate for the increased viscosity of D_2O ($\eta^{rel} = 1.20$). Kinetic data were fit to the Michaelis−Menten equation.

RESULTS

Autophosphorylation of Tie2. Tie2 was activated through an autophosphorylation reaction to produce phospho-Tie2 (pTie2). Using the coupled enzymatic assay in the absence of peptide or protein, the $K_{m,ATP}$ for autophosphorylation was determined to be 712 ± 37 μM. This method did not distinguish between autophosphorylation and ATP hydrolysis but measured the ATP requirement for the combination of these reactions. To achieve high specific activity pTie2, large-scale autophosphorylation reactions were performed at high Tie2 concentration (typically 40 μM), high ATP concentration (10 mM), and low temperature (4 °C). The extent of the reaction was monitored by native isoelectric focusing electrophoresis (IEF) with both coomassie staining for protein (Figure 1A) and [^{32}P]-phosphate incorporation by autoradiography (data not shown). In addition, quantitation of Tie2 activity as a function of autophosphorylation time was performed to optimize the reaction in terms of catalytically relevant autophosphorylation. IEF analysis revealed that the Tie2 kinase domain was a single species with pI = 7.2 (Figure 1A). Limited autophosphorylation shifted Tie2 to a second species with pI = 6.5. Further autophosphorylation shifted Tie2 to a series of species with different pI values (pI = 6.0 to 5.5). The enhancement in catalytic efficiency increased as a function of autophosphorylation time. There was a correlation between appearance of the first phospho-species (pI = 6.5) and a large enhancement in catalytic efficiency. Although sequential phosphorylation events can be inferred by the IEF analysis, the precise assignment of these sites was not possible. As such, the determination of the phosphorylation sites and order of phosphate incorporation was investigated by mass spectrometric analysis.

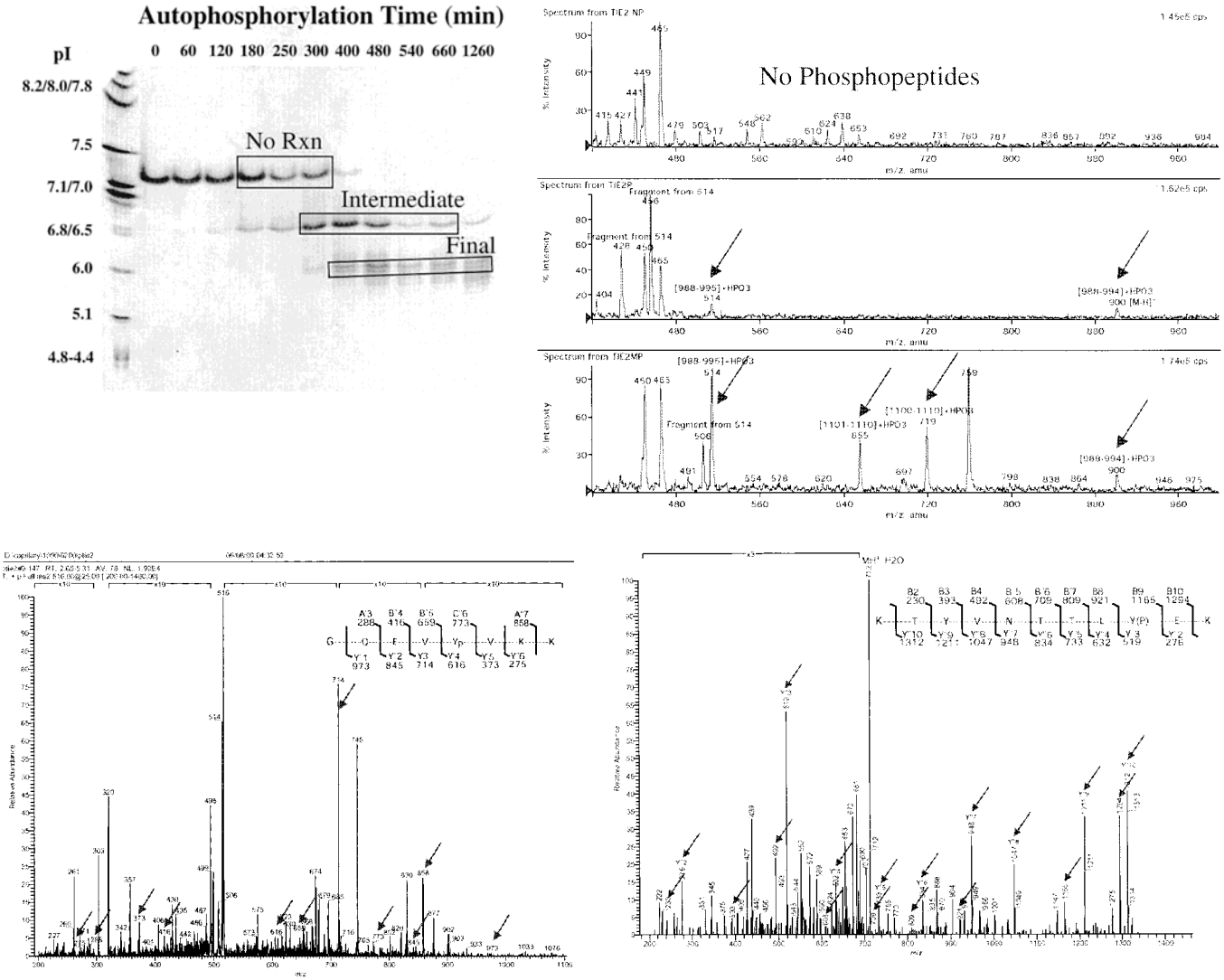

FIGURE 1: Tie2 autophosphorylation proceeds through sequential phosphorylation events. (A) Isoelectric focusing electrophoretic evaluation of a Tie2 autophosphorylation time course shows that initially, Tie2 has a pI = 7.2. The next species formed has a pI = 6.5. Further autophosphorylation shifts Tie2 to a series of bands, pI = 6.0−5.5. The boxed regions indicate slices taken for mass spectrometric analysis. (B) Parent ion scan by nanoESI-MS trypsin of proteolyzed bands. The top spectrum shows that there were no detected phosphopeptides in the absense of the autophosphorylation reaction. The intermediate phosphorylation state of Tie2 is examined in the middle spectrum. One phophopeptide species is observed consistent with Tie2 residues 988−995 from the activation loop. The bottom spectrum shows that more exhaustive autophosphorylation produces an enrichment in the 988−995 phosphopeptide and the appearance of a second phosphopeptide from the C-terminal tail of Tie2 encompassing residues 1101−1110. (C) Microcapillary HPLC-MS/MS sequencing of the activation loop phosphopeptide (988−995) demonstrates that tyrosine residue 992 of the activation loop is phophorylated. (D) Microcapillary HPLC-MS/MS sequencing of the C-terminal phosphopeptide is consistent with phosphorylation of tyrosine residue 1108.

Determination of Phosphorylation Sites on Tie2. A preliminary investigation into the Tie2 autophosphorylation sites was performed with samples of Tie2 and fully phosphorylated Tie2 (pTie2). The samples were proteolyzed with trypsin and subjected to MALDI-TOF mass spectrometry. There were two major phosphorylation sites and one minor site identified. The major phosphopeptides corresponded to Tie2 residues 988−995 (GQEVYVKK) and 1101−1110 (TYVNTTLYEK) while the minor site was 858−869 (KEYASKDDHRDF). Parent ion scans using nano-spray EI mass spectrometry confirmed the identified sites. Tyrosine residues 1102 and 1113 (1101 and 1112 murine sequence) have been reported in the literature to be critical for SH2 domain interactions (*20*−*22*). Tyrosine 992 is predicted to be in the activation loop through sequence alignments (*3*). The third phosphorylation site (858−869) is in the kinase subdomain 2. Multiple sites on Tie2 were shown to be phosphorylated, yet the order of phosphate incorporation was not understood.

To find out the order of phosphate incorporation, a time course of Tie2 autophosphorylation was performed at 4 °C and 5% glycerol to slow the reaction. Isoelectric focusing electrophoresis was used to separate the different Tie2 species (Figure 1A). After trypsin proteolysis of the isolated gel slices, a parent ion scan was performed by nanospray EI mass spectrometry (Figure 1B). No phosphopeptides were detected when Tie2 was not autophosphorylated (apparent pI = 7.2). One phosphopeptide species was detected after moderate autophosphorylation. This peptide was determined to be from the activation loop of Tie2 (apparent pI = 6.5). After further autophosphorylation, a series of bands were identified (multiple bands at apparent pI = 6.0−5.5). The phosphopeptides detected by mass spectrometric analysis were

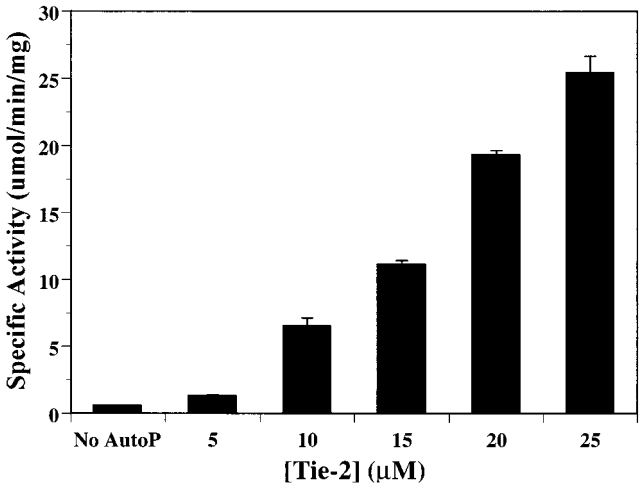

FIGURE 2: The rate of the Tie2 autophosphorylation reaction is dependent on the Tie2 concentration. Tie2 concentration was varied in 4 h, 4 °C autophosphorylation reactions. The resulting Tie2/pTie2 mixture was diluted to 28.6 nM and kinetically monitored in the coupled, enzymatic assay under pseudo V_{max} conditions (2 mM ATP, 11.4 mg/mL poly(Glu_4,Tyr).

consistent with the activation loop peptide and the C-terminal peptide. The relative intensity of the activation loop peptide was greater than the C-terminal peptide. Furthermore, the intensity of the activation loop peptide was greater in the fully autophosphorylated sample relative to the monophosphorylated Tie2 sample. From IEF and MS analysis, the activation loop of Tie2 is autophosphorylated first followed by autophosphorylation of the C-terminal tail. Detailed LC-MS/MS sequencing of the two peptides showed that the autophosphorylation of the activation loop occurs on Tyr992 (Figure 1C) and on Tyr1108 in the C-terminal tail (Figure 1D). IEF and mass spectrometric analysis of the autophosphorylation time course is consistent with a sequential phosphate incorporation: first on the activation loop residue Y992 followed by the C-terminal residue Y1108.

Autophosphorylation can be either an intermolecular (trans mechanism) or intramolecular (cis mechanism) reaction. To investigate the autophosphorylation mechanism of Tie2, the extent of autophosphorylation was probed as a function of Tie2 concentration at a saturating level of ATP (10 mM). For an intramolecular reaction, the normalized reaction rate should be independent of the enzyme concentration. In an intermolecular autophosphorylation mechanism, there should be a dependence on Tie2 concentration because it is both enzyme and substrate. Autophosphorylation reactions were carried out for 4 h at 4° C. Subsequently, Tie2 was diluted to a final concentration of 28.6 nM in a coupled enzymatic assay containing saturating levels of ATP (2 mM) and poly(Glu_4Tyr) (11.4 mg/mL, 16.8 mM) and assayed for activity. As shown in Figure 2, Tie2 specific activity increased as the concentration of Tie2 increased. This result is consistent with an intermolecular trans autophosphorylation mechanism.

Kinetic Analysis of Tie2 and pTie2. The kinetic consequences of the autophosphorylation were investigated. Tie2 and pTie2 activities were evaluated in two distinct and complementing assay formats. Autophosphorylation of Tie2 was shown to occur on Tyr992 in the activation loop and enhances the kinase specific activity. A coupled, enzymatic assay format (CE format) was used to measure ADP production. Tie2-catalyzed production of ADP from ATP that accompanied phosphate transfer to the random copolymer poly(Glu_4Tyr) was coupled to the oxidation of NADH through the sequential activities of pyruvate kinase (PK) and lactate dehydrogenase (LDH). NADH conversion to NAD^+ was monitored spectrophotometrically by the decrease in absorbance at 340 nm ($\epsilon = 6.22\ cm^{-1}\ mM^{-1}$). A second assay format was used to measure the production of [^{32}P]-labeled phospho-protein (histone 2B). Histone 2B is the substrate for Tie2 in the coupled enzymatic format and in a glass fiber filterplate assay format. The $K_{m,Histone\ 2B}$ was determined to be 8.8 ± 2.6 μM in the coupled, enzymatic format at 2 mM ATP and 4.0 ± 0.9 μM in the glass fiber filterplate format at 0.1 mM ATP. [^{32}P]-Phosphate labeling studies of histone 2B with pTie2 were consistent with only one phosphate being incorporated per molecule of histone 2B (data not shown). Mass spectrometry analysis (MALDI-TOF and NanoESI mass spectrometry) of exhaustively phosphorylated histone 2B revealed one dominant phosphorylation (residues 35−43). This phosphopeptide contains three tyrosine residues (ESYSVYVYK). Detailed LC-MS/MS showed that the third tyrosine (ESYSVYVpYK) of the peptide is the dominant phosphorylation site for pTie2 with the second tyrosine as a secondary site. Under the kinetic control used in the filtermate assay, only one phosphate should be incorporated per molecule of histone 2B. Interesting, this site is not the predicted phosphorylation site (by a NetPhos computational algorithm). The filtermate assay format is as follows: kinase reactions run with γ-[^{32}P]-ATP, histone 2B phosphoacceptor, terminated with trichloroacetic acid, and isolated on glass fiber 96-well filterplates. By both assay formats/conditions, autophosphorylation of Tie2 caused a >100-fold enhancement in both turnover number (k_{cat}) and specificity constant (k_{cat}/K_m) independent of assay format and phosphoacceptor (poly(Glu_4Tyr) or histone 2B (Table 1). Minor 2- to 4-fold changes in substrate K_m values between Tie2 and pTie2 were observed. As determined in multiple assays with multiple phosphoacceptor substrates, autophosphorylation transformed Tie2 into a much more potent catalyst (pTie2).

Table 1: Autophosphorylation of Tie2 Enhances Its Catalytic Efficiency[a]

	unphosphorylated Tie2			phospho-Tie2		
	K_m (μM)	k_{cat} (s^{-1})	k_{cat}/K_m ($s^{-1}M^{-1}$)	K_m (μM)	k_{cat} (s^{-1})	k_{cat}/K_m ($s^{-1}M^{-1}$)
MgATP	366 ± 28	0.442 ±0.008	1210	73.9 ± 11.0	51.0 ± 2.8	690 000
poly(Glu_4Tyr)	9000 ± 354		49.1	4770 ± 735		10 700
histone 2B	4.40 ± 0.90	0.0020 ± 0.0003	455	1.71 ± 0.09	0.457 ± 0.015	267 000

[a] The observed enhancement was independent of phosphoacceptor and assay format as measured by steady-state kinetic constants for Tie2 and autophosphorylated Tie2. The coupled enzymatic analysis of Tie2 processing of ATP and poly(Glu_4Tyr) were measured at 37 °C. Variable substrate concentration was measured at a fixed saturating concentration of the other substrate. Tie2 mediated processing of histone 2B was measured in the filtermate assay at 100 μM ATP and 21 °C.

pH-Stability and pH-Rate Studies. Autophosphorylation has a dramatic effect on Tie2 catalytic efficiency. Is there an autophosphorylation-dependent change in the pK_a values for ionizable residues? To ensure valid pH−rate results, pH-

Table 2: pH−Rate Behavior for Tie2 and Autophosphorylated Tie2 (pTie2)[a]

	Tie2		pTie2	
method	pK_{a1}	pK_{a2}	pK_{a1}	pK_{a2}
pH−rate k_{cat}	7.2	10.1	6.5	9.4
pH−rate k_{cat}/K_m	7.1	>10	6.2	9.4
pH−activity	7.4	10.5	6.6	9.1

[a] Tie2 autophosphorylation shifts the pK_a values of the catalytically relevant ionizable residues. pH-Activity profiles were performed at fixed substrate concentrations: 100 μM ATP and 8 μM histone 2B.

Table 3: Inhibition of Tie2 and PTie2 by Known ATP-competitive Kinase Inhibitors[a]

kinase inhibitor	Tie2 K_i (μM)	pTie2 K_i (μM)
staurosporine	0.121 ± 0.024	0.152 ± 0.015
K252a	0.90 ± 0.20	0.573 ± 0.020
SB203580	14.7 ± 0.9	40.9 ± 5.5
PP2	9.18 ± 1.17	28.4 ± 5.4
damnacanthal	4.00 ± 0.45	7.76 ± 0.77
H-89	>30	>30
bisindolylmaleimide I	>30	>30

[a] ATP-competitive kinase inhibitors have a wide range of potencies toward Tie2 and PTie2. In general, Tie2 was modestly easier to inhibit relative to pTie2. To get measurable kinase activities, the concentrations of Tie2 and pTie2 were chosen to be 610 and 20 nM, respectively.

stability profiles for both Tie2 and activated Tie2 (pTie2) were performed. Stability to different pH conditions was evaluated by pH swap experiments. Exposure of pTie2 to pH conditions from 5.5 to 9.5 prior to kinetic analysis at pH 7.5 did not have a significant effect on the final k_{cat} values (14.7 ± 1.6 s^{-1}) nor on the k_{cat}/K_m values (2320 ± 360 s^{-1} M^{-1}). This experiment shows that pTie2 is resistant to irreversible denaturation in the examined pH range. In a parallel study, Tie2 did not exhibit pH-dependent instabilities. Preexposure of Tie2 to a 5.5−9.5 range of pH conditions did not significantly affect the k_{cat} values at pH 7.5 (0.48 ± 0.03 s^{-1}) or the k_{cat}/K_m values (68.2 ± 12.3 s^{-1} M^{-1}). Both Tie2 and pTie2 were shown to be stable to irreversible pH denaturation in the examined pH range.

After the pH-stabilities of Tie2 and pTie2 had been established, the pH−rate behaviors were characterized (Figure 3). The MES and bis-tris propane buffer scheme described in the stability study was used in conjunction with the radioactive filtermate assay (to avoid pH effects on the coupling enzymes). pH−activity profiles (fixed substrate concentrations) and pH−rate profiles (variable histone 2B concentrations) were performed for both Tie2 and pTie2. Both the pH−activity profiles and the pH−rate profiles for Tie2 and pTie2 were bell-shaped with two apparent pK_a values. The results are summarized in Table 2. Autophosphorylation of Tie2 to pTie2 causes the catalytically relevant pK_a values to decrease. For example, the Tie2 pH−k_{cat} profile had pK_a values of 7.2 and 10.1, while pTie2 had pK_a values of 6.5 and 9.2. A similar shift in pK_a values was observed for the pH−k_{cat}/K_m profiles. Autophosphorylation of Tie2 affects a change in pK_a of catalytically relevant ionizable Tie2 residues.

Viscosity Studies of Tie2 and pTie2. Viscosity effects on an enzymatic rate have been used to measure the contribution of physical steps (e.g., product dissociation) to the overall reaction rate (Figure 4). Viscosity studies of Tie2 and pTie2

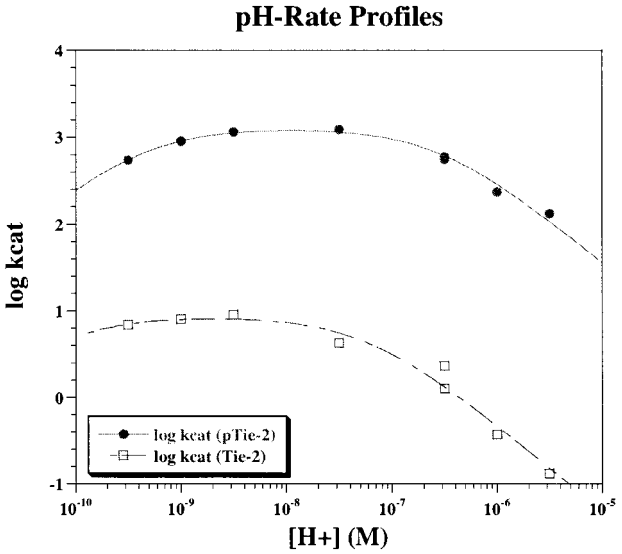

FIGURE 3: Autophosphorylation perturbs the pK_a values of catalytically relevant ionizable residues. pH−rate profiles for Tie2 and pTie2 were performed with filtermate assay format to avoid pH effects on coupling enzymes. Analysis of the k_{cat} data revealed two pK_a values for pTie2 (6.5 and 9.4), while Tie2 had two different pK_a values (7.1 and 10.1). Autophosphorylation of Tie2 had a modest but significant effect on the catalytically relevant ionizable residues of Tie2.

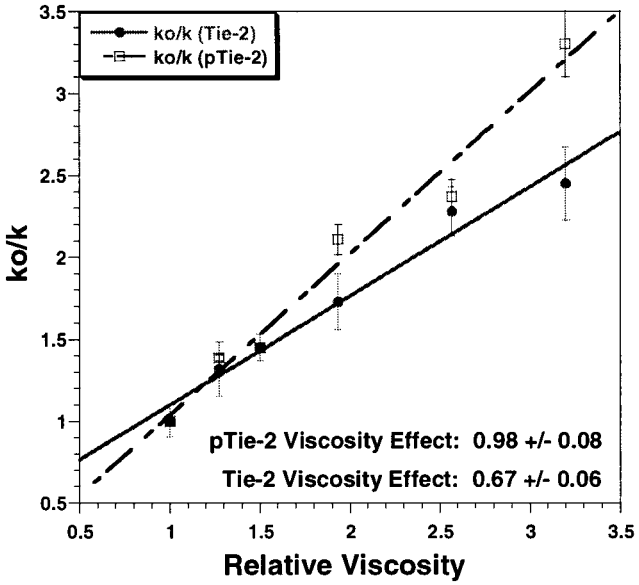

FIGURE 4: Viscosity studies of Tie2 and pTie2 show that autophosphorylation makes product dissociation more rate-limiting. The sucrose microviscogen had a effect on the reaction rates for both Tie2 and pTie2. The magnitude of the effect was much larger for pTie2 (0.98 ± 0.08) as compared to Tie2 (0.67 ± 0.06). Macroviscogen controls confirmed that the observed effects were due to the variable microviscosity.

were used to investigate whether the large observed rate enhancement had an effect on the contribution of physical steps toward the overall reaction rate. At saturating ATP concentrations, the kinetic mechanism of Tie2 can be simplified (eq 3). The $(k_{cat})^{\eta}$ is the measure of the ratio of

$$E\cdot ATP + S \underset{k_{-2}}{\overset{k_2}{\rightleftharpoons}} E\cdot ATP\cdot S \xrightarrow{k_3} E\cdot ADP\cdot P \xrightarrow{k_4} E + ADP + P \quad (3)$$

the chemical rate constant (k_3) and the product release rate

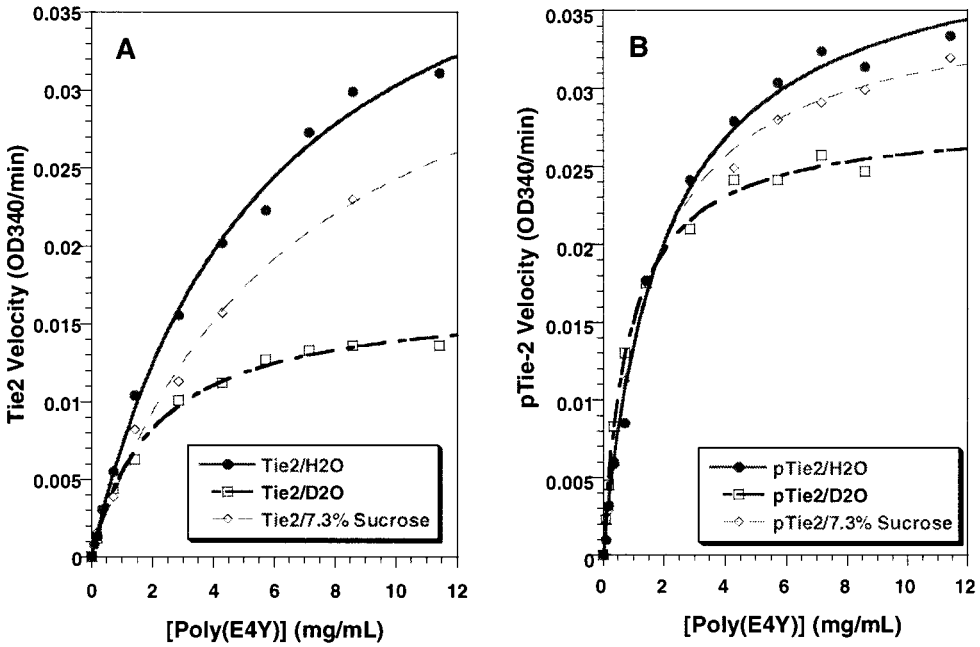

FIGURE 5: Solvent isotope studies of Tie2 and pTie2 show that autophosphorylation causes the chemical step to be less rate limiting. The $(k_{cat})^D$ shifts from 2.42 ± 0.12 for Tie2 to 1.28 ± 0.04 for pTie2. The sucrose viscosity control was used to normalize for the higher viscosity of D_2O.

(k_4): $(k_{cat})^\eta = k_3/(k_3 + k_4)$. The value of $(k_{cat})^\eta$ approaches unity as the rate of the chemistry step becomes large with respect to the rate of product release. Viscosity effects can be observed by measuring changes in the specificity constants (k_{cat}/K_m) of Tie2 and pTie2 (Figure 4). The $(k_{cat}/K_m)^\eta$ is a measure of the ratio of the chemistry step (k_3) to substrate dissociation rate (k_{-2}): $(k_{cat}/K_m)^\eta = k_3/(k_{-2} + k_3)$. When $(k_{cat}/K_m)^\eta = 1$, then substrate dissociation is rate limiting. Conversely, if $(k_{cat}/K_m)^\eta = 0$, then chemistry (k_3) is solely rate limiting.

The effects of microviscogen (sucrose) and macroviscogen (PEG 8000) were measured for both Tie2 and pTie2. Reactions were performed at 24 °C with saturating ATP (2 mM) and variable poly(Glu_4Tyr) as the phosphoacceptor. No macroviscogen effect was observed for either Tie2 or pTie2 (data not shown). Microviscogen effects were observed for both Tie2 and pTie2. When $(k_{cat})^\eta = 1$, product release is fully rate-limiting and when $(k_{cat})^\eta = 0$, product release is not rate-limiting. pTie2 showed an near complete viscosity effect ($(k_{cat})^\eta = 0.94 \pm 0.08$), while for unactivated Tie2 product release was partially rate-limiting ($(k_{cat})^\eta = 0.67 \pm 0.06$). The $(k_{cat}/K_m)^\eta$ viscosity effect for Tie2 was determined to be 0.74 ± 0.08 and 0.90 ± 0.14 for pTie2. Autophosphorylation had a significant effect on the contribution of product ($(k_{cat})^\eta$) and substrate ($(k_{cat}/K_m)^\eta$) release to the overall rate.

Individual rate constants and dissociation constants for Tie2 under saturating ATP concentration (eq 3) can be calculated from the equations for $(k_{cat})^\eta$, $(k_{cat}/K_m)^\eta$, $k_{cat}[k_3k_4/(k_3 + k_4)]$, and $k_{cat}/K_m[k_2k_3/(k_{-2} + k_3)]$ (*48*). The simplified equations are as follows: $k_4 = k_{cat}/(k_{cat})^\eta$, $k_3 = k_{cat}/(1 - (k_{cat})^\eta)$, $k_2 = (k_{cat}/K_m)/(k_{cat}/K_m)^\eta$, $k_{-2} = [(k_3/(k_{cat}/K_m)^\eta - k_3]$, and $K_{d,PGT} = [K_{m,PGT}(1 - (k_{cat}/K_m)^\eta)]/(1 - (k_{cat})^\eta)$. The dissociation constant for poly(Glu_4Tyr) ($K_{d,PGT}$) did not change significantly as a function of the phosphorylation state of Tie2: 7.09 mM (Tie2) and 7.97 mM (pTie2). A large autophosphorylation effect was observed on the chemistry step (k_3): 1.34 s^{-1} (Tie2) and 850 s^{-1} (pTie2). Product release (k_4) was enhanced for pTie2 (54 s^{-1}) as compared to Tie2 (0.66 s^{-1}). The phosphoacceptor on-rates (k_2) and off-rates (k_{-2}) are as follows: Tie2 (k_2 = 66.4 s^{-1} M^{-1}, k_{-2} = 0.47 s^{-1}) and pTie2 (k_2 = 11 900 s^{-1} M^{-1}, k_{-2} = 94.0 s^{-1}). Detailed kinetic analysis of Tie2 and pTie2 demonstrates that the major effect of autophosphorylation is on the chemistry step.

Kinetic Isotope Effects on Tie2 and pTie2. Solvent isotope effects (SIE) of deuterium oxide have been used to gauge the contribution of the chemical step (e.g., phosphate transfer) to the overall reaction rate (Figure 5). SIE studies were used as a complement to the viscosity studies because the SIE can probe the relative contribution of the chemical step toward the overall reaction rate. Kinetic measurements were performed in the coupled enzymatic assay system at 37 °C with saturating ATP and variable poly(Glu_4Tyr). A 7.3% sucrose solution was used as a viscosity control to normalize for the viscosity of D_2O ($\eta^{rel} = 1.2$). No isotope effect was measured on the coupling enzyme system. After normalizing for viscosity effects, pTie2 displayed a modest $(k_{cat})^H/(k_{cat})^D$ solvent isotope effect (1.28 ± 0.04) while Tie2 had a large $(k_{cat})^H/(k_{cat})^D$ solvent isotope effect (2.42 ± 0.12). In the complementary filtermate assay format (γ-[^{32}P]-ATP, 0.1 mM ATP, variable histone 2B) pTie2 displayed a $(k_{cat})^H/(k_{cat})^D$ solvent isotope effect (1.37 ± 0.08), which was statistically identical to the value derived from the coupled enzymatic assay. Large D_2O SIE were observed on K_m values for poly(Glu_4Tyr) which could be expected for an equilibrium isotope effect. For Tie2, the K_m^H/K_m^D effect was determined to be 2.73 ± 0.29, while for pTie2 the observed K_m^H/K_m^D was 2.33 ± 0.22. There was no large $(k_{cat}/K_m)^H/(k_{cat}/K_m)^D$ SIE observed for either Tie2 or pTie2. The $(k_{cat}/K_m)^H/(k_{cat}/K_m)^D$ SIE was observed to be 1.04 ± 0.11 for Tie2 and 0.62 ± 0.06 for pTie2. The solvent isotope studies are consistent with the chemistry step being less rate-limiting after Tie2 has undergone autophosphorylation.

Inhibition Studies of Tie2 and pTie2. A panel of known reversible ATP-competitive kinase inhibitors was assembled to probe the Tie2 active site for autophosphorylation-dependent changes (Table 3). The ATP binding cleft between the two kinase domains is large, and kinase inhibitors are known to bind to different regions. The panel included the general kinase inhibitor staurosporine and its analogue K252a. Inhibitors of protein kinases were chosen: damnacanthal (p56Lck tyrosine kinase), PP2 (src family tyrosine kinases), (p38 S/T kinase), bisindolymaleimide I (PKA, PKC), and H-89 (PKA S/T kinase). The ATP-competitive kinase inhibitors had a large range of potencies against both Tie2 and pTie2. The inhibition of specific inhibitors toward Tie2 and pTie2 was comparable, but a trend was observed. Most of the compounds inhibited Tie2 more potently than pTie2 (except K252a). To ensure that the kinase inhibitors had no effect on the coupling enzymes, the filtermate assay was performed for inhibition of pTie2. The inhibitor potencies determined in the filtermate assay were in agreement with the results determined in the coupled, enzymatic assay. ATP-competitive inhibitors demonstrated strong kinase family selectivity and moderate phosphorylation-state selectivity.

DISCUSSION

Autophosphorylation Sites and Order of Autophosphorylation. Receptor autophosphorylation is an essential event in many signal transduction pathways and is known to have multiple functions in vivo including activation of the kinase domain and creation of recruitment sites for downstream signaling molecules. For many RTKs, multiple sites are phosphorylated, and the order of phosphorylation of these sites can be either random or sequential. The current studies show that in our Tie2 construct autophosphorylation occurs first in the activation loop followed by autophosphorylation of the C-terminal tail. Receptor kinase domains are usually activated by phosphorylation of a tyrosine residue in the activation loop (*49*). Sequence homology studies have shown that there is a consensus sequence for the activation loop (*3*) and the predicted site for Tie2 is Y992. Mass spectrometric studies of autophosphorylated Tie2 showed that this site is indeed autophosphorylated. The recent structural study of Tie2 kinase domain reported that autophosphorylation of wild-type Tie2 at Y992 was not possible (*18*). Furthermore, they report that the triple mutant (Y897, Y1048, S1119) was able to be autophosphorylated at Y992. The present study shows that phosphorylation of wild-type Tie2 is facile. The simplest explanation for the discrepancy is that through the course of the protein purification phosphates were either incorporated or removed from Tie2. The present studies show that phosphorylation of these sites (Y897, Y1048, S1119) is minor at best. An alternate explanation is that other kinase(s) regulate Tie2 through phosphorylation of these residues. Nonetheless, our studies show that autophosphorylation of the activation loop residue Y992 occurs first and its phosphorylation is facile.

Another role of autophosphorylation is to create docking sites for Src Homology 2 (SH2) and phosphotyrosine binding (PTB) domains though phosphorylation of C-terminal tyrosine residues. The C-terminal tail of Tie2 has been reported to be critical for recruitment of downstream signaling molecules through yeast two-hybrid and in vitro association studies (*20*−*22*, *25*). Yeast two-hybrid studies with either Tie2 kinase domain or its kinase-inactive mutant as bait showed associations with SH2-containing molecules in a phospho-specific manner (*21*, *22*). In vitro association studies have also been used to demonstrate an autophosphorylation-specific interaction of Tie2 with SH2-containing proteins (*20*−*22*). The precise assignment of the C-terminal recruitment site for SH2-containing proteins remains controversial. Tyrosine residues 1101 and/or 1112 (murine sequence; 1102 and 1113 for our sequence) have been reported to be the docking sites for SH2-containing signaling molecules (*20*−*22*, *25*); however, we did not observe phosphorylation of these residues. A phosphopeptide containing the C-terminal site identified in the present study was shown by others using a BIAcore association approach to associate more tightly to the Grb14 SH2 domain than phosphopeptides containing Y1101 or 1112 (*22*). A recent structural study did not find evidence for phosphorylation of either Y1101 or 1112 (*18*). The present study conclusively shows through detailed mass spectrometric analysis that the Tie2 intracellular domain autophosphorylates its C-terminal tail on Y1108. There are multiple explanations for the discrepancies between the literature studies and the current mass spectrometric analysis. (i) The in vitro autophosphorylation conditions used herein may not be physiologically relevant. The true effective concentration of Tie2 kinase domains due to the receptor dimerization is not known but may be higher than the simple concentration of Tie2 in the membrane. (ii) Mutagenesis of Y1101 and Y1112 affects the local conformation and prevents the autophosphorylation. (iii) In vitro association studies of Tie2 C-terminal tyrosine mutants may not be conclusive because many of the studies show that they modulate but totally abrogate interactions with SH2-containing proteins (iv) Tie2 C-terminal mutants may alter the stability of the Tie2. There is literature precedence for sequential autophosphorylation events. The insulin receptor has been shown to autophosphorylate in the activation loop on three tyrosine residues (*50*). Concomitant with the third phosphate incorporation into the activation loop, phosphorylation of two C-terminal sites are observed (*50*). The Tie2 receptor is a simpler system with only one required phosphorylation event in the activation loop apparently necessary for activation. Nonetheless, the current study uses mass spectrometric analysis of a well-characterized autophosphorylation reaction time course to show a sequential autophosphorylation of Tie2 at Y992 in the activation loop first followed by Y1108 in the C-terminal tail.

Kinetic Analysis of Tie2 and pTie2. The autophosphorylation can be either cis (intramolecular) or trans (intermolecular). In the trans mechanism, the receptor dimerization increases the effective concentration of the kinase domains which enhances the reaction rate. The Tie2 autophosphorylation rate is dependent on the concentration of Tie2. This observation is consistent with a trans autophosphorylation mechanism. Other RTK such as the insulin receptor (*51*, *52*) and VEGF receptor (*46*) have been shown to have a trans mechanism for autophosphorylation of the activation loop.

Kinetic analysis of unphosphorylated and autophosphorylated Tie2 was undertaken to probe the overall effect of autophosphorylation on the effectiveness and efficiency of Tie2 as a catalyst. The effect of autophosphorylation resides predominantly on k_{cat}. The k_{cat} effect is independent of phosphoacceptor (peptide, protein, and random copolymer).

Furthermore, the rate enhancement is increased by 2 orders of magnitude. Tie2 autophosphorylation had only a minor effect on the $K_{m,ATP}$ value. Autophosphorylation causes a rate enhancement for other tyrosine kinases, but the magnitude varies widely: no effect for EGF receptor (*53*), modest effect on the HER-2 receptor (*54*), 2.5-fold k_{cat} enhancement for VEGF receptor (*46*), 7-fold V_{max} enhancement of c-Met (*55*), a 7-fold increase in k_{cat} of the insulin receptor (*56*), and 42-fold increase in k_{cat} of v-Fps (*57*). The combination of the large rate enhancement upon Tie2 activation and the measurable reaction rate of the unactivated receptor made Tie2 an ideal system for investigating the mechanistic effects of autophosphorylation on catalysis.

pH-Rate Profiles. The effect of pH on catalysis is one of the classic methods for studying enzyme mechanism. Although pH−rate studies have been performed for many protein kinases, the effect of kinase activation on the pH−rate profiles remains obscure. pH−Rate studies of Tie2 and pTie2 reveal a > 0.5 unit shift in catalytic pK_a values. This shift in pK_a may have its root in a local environment change around the ionizable residues due to autophosphorylation-induced local and global conformational changes. For kinases, enzymatic catalysis occurs in the cleft between the N- and C-terminal domains. The rotation of the N-terminal domain with respect to the C-terminal domain has been well documented (*5*, *58*) and may play a role in the observed pK_a differences. Autophosphorylation of Tie2 changes the ionization potential of catalytically relevant residues.

Viscosity Studies. The contribution of physical steps to the overall reaction rate of kinases has been reported for individual kinase activation states (*32*, *36*, *39*, *59*). A limited number of kinases have been studied in terms of the effect of autophosphorylation on the mechanism: insulin receptor, v-Fps, and HER-2. Autophosphorylation has different effects on these two kinases. X-ray structure analysis of the related insulin receptor indicates that the activation loop phosphorylation alters the substrate access to the active-site cleft (*52*). Kinetic studies of the insulin receptor confirm that the phosphoacceptor substrate dissociation constant is enhanced 10-fold through autophosphorylation (*56*). Our studies on Tie2 show almost no effect on the phosphoacceptor dissociation constant and a large effect on the chemistry step rate. A similar observation has been reported for the nonreceptor tyrosine kinase v-Fps (*57*). Autophosphorylation of HER-2 receptor tyrosine kinase was shown by transient kinetic analysis to primarily affect product release with little impact on the chemistry step (*54*). Nonetheless, autophosphorylation of Tie2 enhances its catalytic efficiency by making the chemical step less rate-limiting than product release or substrate binding. One of the tenets of the concept of catalytic perfection championed by Albery and Knowles is that as an enzyme approaches catalytic perfection, internal steps/states (Michaelis complexes, transition state) are no longer rate limiting, and external steps (substrate capture, product release) become rate limiting (*60*, *61*). For Tie2, autophosphorylation makes product release almost exclusively rate limiting and more perfect.

Solvent Isotope Studies. Solvent isotope studies are a good complement to viscosity studies because they can measure the contribution of proton transfer (chemical step) to the overall reaction rate (*62*). Analysis of solvent isotope effects (SIE) is complicated due to the compound effects of deuterium oxide on both rates and equilibrium constants. Adams has reported a thorough treatment of isotope theory applied to the tyrosine kinase v-Fps (*40*). At a saturating ATP concentration, the Tie2 reaction can be simplified (eq 4). Normal k_{cat} isotope effects for both Tie2 and pTie2 were observed, although the magnitude was significantly different. Solvent isotope effects on k_{cat} can be utilized to compare the contribution of phosphate transfer (chemical step) to the overall reaction rate relative to the release the products from the active site (physical steps). The observed isotope effect on k_{cat} was more pronounced for Tie2 relative to pTie2 which is consistent with a higher transition-state energy. SIE effects on K_m were observed for both forms of Tie2 and were of comparable magnitudes. Similar K_m SIE effects were observed for Src kinase processing of poly(Glu_4Tyr) (*36*) and v-Fps kinase processing of peptides (*40*). The simplest explanation of the K_m SIE is an equilibrium isotope effect that alters substrate binding. No significant normal k_{cat}/K_m isotope effect was observed for either form of Tie2. The lack of a k_{cat}/K_m SIE may be due to offsetting kinetic (k_{cat}) and equilibrium (K_m) isotope effects. Nonetheless, the kinetic isotope effects on k_{cat} clearly show that autophosphorylation of Tie2 makes the chemical step significantly less rate-limiting.

Autophosphorylation alters Tie2 to make diffusion steps in the enzyme mechanism more rate-limiting. This shift in rate-limiting step(s) will alter the distribution of enzyme species along the reaction coordinates. As observed in the inhibition studies with the ATP-competitive kinase inhibitors, pTie2 was more difficult to inhibit. It is tempting to speculate that since the majority of pTie2 will be complexed with products (e.g., ADP), the lower susceptibility to inhibition is due to a lower probability of an inhibitor encountering an unoccupied ATP binding site. Other significant considerations such as different conformations or inhibitor-induced changes may dominate the susceptibility to inhibition. Future kinetic studies of potent specific inhibitors of Tie2 coupled to structural studies will address the effect of autophosphorylation on inhibitor specificity.

In summary, the studies described here provide some of the mechanistic details of tyrosine kinase autophosphorylation which complements the multitude of biological and structural studies of protein kinases. To date, the described series of experiments illustrate a consistent picture of the mechanistic consequences of kinase autophosphorylation. For this critical angiogenic receptor tyrosine kinase, autophosphorylation changes the environment around catalytically relevant ionizable residues to perturb their pK_a values. Autophosphorylation dramatically enhances the catalytic efficiency by several orders of magnitude and makes the enzyme diffusion steps more rate-limiting. These changes drive Tie2 to become the more catalytically perfect pTie2.

ACKNOWLEDGMENT

We gratefully acknowledge Cris Lewis for critically reading the manuscript and offering valued opinions. We also thank Camran Parast for his input at various stages of the work.

REFERENCES

1. van der Geer, P., Hunter, T., and Lindberg, R. A. (1994) *Annu. Rev. Cell. Biol. 10,* 251−337.

2. Heldin, C. H. (1995) *Cell 80*, 213−23.
3. Hanks, S. K., and Hunter, T. (1995) *FASEB J. 9*, 576−96.
4. Williams, J. C., Wierenga, R. K., and Saraste, M. (1998) *Trends Biochem. Sci. 23*, 179−84.
5. Hubbard, S. R. (1999) *Prog. Biophys. Mol. Biol. 71*, 343−58.
6. Tallquist, M. D., Soriano, P., and Klinghoffer, R. A. (1999) *Oncogene 18*, 7917−32.
7. Holash, J., Wiegand, S. J., and Yancopoulos, G. D. (1999) *Oncogene 18*, 5356−62.
8. Hagedorn, M., and Bikfalvi, A. (2000) *Crit. Rev. Oncol. Hematol. 34*, 89−110.
9. Dumont, D. J., Yamaguchi, T. P., Conlon, R. A., Rossant, J., and Breitman, M. L. (1992) *Oncogene 7*, 1471−80.
10. Dumont, D. J., Gradwohl, G. J., Fong, G. H., Auerbach, R., and Breitman, M. L. (1993) *Oncogene 8*, 1293−301.
11. Maisonpierre, P. C., Goldfarb, M., Yancopoulos, G. D., and Gao, G. (1993) *Oncogene 8*, 1631−7.
12. Sato, T. N., Qin, Y., Kozak, C. A., and Audus, K. L. (1993) *Proc. Natl. Acad. Sci. U.S.A. 90*, 9355−8.
13. Schnurch, H., and Risau, W. (1993) *Development 119*, 957−68.
14. Ziegler, S. F., Bird, T. A., Schneringer, J. A., Schooley, K. A., and Baum, P. R. (1993) *Oncogene 8*, 663−70.
15. Davis, S., Aldrich, T. H., Jones, P. F., Acheson, A., Compton, D. L., Jain, V., Ryan, T. E., Bruno, J., Radziejewski, C., Maisonpierre, P. C., and Yancopoulos, G. D. (1996) *Cell 87*, 1161−9.
16. Maisonpierre, P. C., Suri, C., Jones, P. F., Bartunkova, S., Wiegand, S. J., Radziejewski, C., Compton, D., McClain, J., Aldrich, T. H., Papadopoulos, N., Daly, T. J., Davis, S., Sato, T. N., and Yancopoulos, G. D. (1997) *Science 277*, 55−60.
17. Valenzuela, D. M., Griffiths, J. A., Rojas, J., Aldrich, T. H., Jones, P. F., Zhou, H., McClain, J., Copeland, N. G., Gilbert, D. J., Jenkins, N. A., Huang, T., Papadopoulos, N., Maisonpierre, P. C., Davis, S., and Yancopoulos, G. D. (1999) *Proc. Natl. Acad. Sci. U.S.A. 96*, 1904−9.
18. Shewchuk, L. M., Hassell, A. M., Ellis, B., Holmes, W. D., McKee, D. D., and Moore, J. T. (2000) *Structure 8*, 1105−1113.
19. Dumont, D. J., Gradwohl, G., Fong, G. H., Puri, M. C., Gertsenstein, M., Auerbach, A., and Breitman, M. L. (1994) *Genes Dev. 8*, 1897−909.
20. Huang, L., Turck, C. W., Rao, P., and Peters, K. G. (1995) *Oncogene 11*, 2097−103.
21. Kontos, C. D., Stauffer, T. P., Yang, W. P., York, J. D., Huang, L., Blanar, M. A., Meyer, T., and Peters, K. G. (1998) *Mol. Cell. Biol. 18*, 4131−40.
22. Jones, N., Master, Z., Jones, J., Bouchard, D., Gunji, Y., Sasaki, H., Daly, R., Alitalo, K., and Dumont, D. J. (1999) *J. Biol. Chem. 274*, 30896−905.
23. Vikkula, M., Boon, L. M., Carraway, K. L., 3rd, Calvert, J. T., Diamonti, A. J., Goumnerov, B., Pasyk, K. A., Marchuk, D. A., Warman, M. L., Cantley, L. C., Mulliken, J. B., and Olsen, B. R. (1996) *Cell 87*, 1181−90.
24. Calvert, J. T., Riney, T. J., Kontos, C. D., Cha, E. H., Prieto, V. G., Shea, C. R., Berg, J. N., Nevin, N. C., Simpson, S. A., Pasyk, K. A., Speer, M. C., Peters, K. G., and Marchuk, D. A. (1999) *Hum. Mol. Genet. 8*, 1279−89.
25. Jones, N., and Dumont, D. J. (1998) *Oncogene 17*, 1097−108.
26. Qamar, R., and Cook, P. F. (1993) *Biochemistry 32*, 6802−6.
27. Zheng, J., Knighton, D. R., ten Eyck, L. F., Karlsson, R., Xuong, N., Taylor, S. S., and Sowadski, J. M. (1993) *Biochemistry 32*, 2154−61.
28. Gibbs, C. S., Knighton, D. R., Sowadski, J. M., Taylor, S. S., and Zoller, M. J. (1992) *J. Biol. Chem. 267*, 4806−14.
29. Whitehouse, S., Feramisco, J. R., Casnellie, J. E., Krebs, E. G., and Walsh, D. A. (1983) *J. Biol. Chem. 258*, 3693−701.
30. Cook, P. F., Neville, M. E., Jr., Vrana, K. E., Hartl, F. T., and Roskoski, R., Jr. (1982) *Biochemistry 21*, 5794−9.
31. Kong, C.-T., and Cook, P. F. (1988) *Biochemistry 27*, 4795−4799.
32. Adams, J. A., and Taylor, S. S. (1992) *Biochemistry 31*, 8516−22.
33. Zhou, J., and Adams, J. A. (1997) *Biochemistry 36*, 2977−84.
34. Yoon, M. Y., and Cook, P. F. (1987) *Biochemistry 26*, 4118−25.
35. Grant, B. D., and Adams, J. A. (1996) *Biochemistry 35*, 2022−2029.
36. Cole, P. A., Burn, P., Takacs, B., and Walsh, C. T. (1994) *J. Biol. Chem. 269*, 30880−7.
37. Grace, M. R., Walsh, C. T., and Cole, P. A. (1997) *Biochemistry 36*, 1874−81.
38. Sondhi, D., Xu, W., Songyang, Z., Eck, M. J., and Cole, P. A. (1998) *Biochemistry 37*, 165−72.
39. Wang, C., Lee, T. R., Lawrence, D. S., and Adams, J. A. (1996) *Biochemistry 35*, 1533−9.
40. Adams, J. A. (1996) *Biochemistry 35*, 10949−56.
41. Liu, X., and Pawson, T. (1994) *Recent Prog. Horm. Res. 49*, 149−60.
42. Cobb, M. H., Sang, B. C., Gonzalez, R., Goldsmith, E., and Ellis, L. (1989) *J. Biol. Chem. 264*, 18701−6.
43. Ullrich, A., and Schlessinger, J. (1990) *Cell 61*, 203−12.
44. Wei, L., Hubbard, S. R., Hendrickson, W. A., and Ellis, L. (1995) *J. Biol. Chem. 270*, 8122−30.
45. Mohammadi, M., Schlessinger, J., and Hubbard, S. R. (1996) *Cell 86*, 577−87.
46. Parast, C. V., Mroczkowski, B., Pinko, C., Misialek, S., Khambatta, G., and Appelt, K. (1998) *Biochemistry 37*, 16788−801.
47. Shoemaker, D. P., and Garland, C. W. (1962) *Exp. Phys. Chem.*, 2nd ed., McGraw-Hill, New York.
48. Konkol, L., Hirai, T. J., and Adams, J. A. (2000) *Biochemistry 39*, 255−262.
49. Hubbard, S. R., and Till, J. H. (2000) *Annu. Rev. Biochem. 69*, 373−98.
50. White, M. F., Shoelson, S. E., Keutmann, H., and Kahn, C. R. (1988) *J. Biol. Chem. 263*, 2969−80.
51. Hubbard, S. R., Wei, L., Ellis, L., and Hendrickson, W. A. (1994) *Nature 372*, 746−54.
52. Hubbard, S. R. (1997) *EMBO J. 16*, 5572−81.
53. Gotoh, N., Tojo, A., Hino, M., Yazaki, Y., and Shibuya, M. (1992) *Biochem. Biophys. Res. Commun. 186*, 768−74.
54. Jan, A. Y., Johnson, E. F., Diamonti, A. J., Carraway, K. L., and Johnson, K. S. (2000) *Biochemistry 39*, 9786−9803.
55. Naldini, L., Vigna, E., Ferracini, R., Longati, P., Gandino, L., Prat, M., and Comoglio, P. M. (1991) *Mol. Cell. Biol. 11*, 1793−803.
56. Ablooglu, A. J., and Kohanski, R. A. (2001) *Biochemistry 40*, 504−513.
57. Saylor, P., Hanna, E., and Adams, J. A. (1998) *Biochemistry 37*, 17875−17881.
58. Goldsmith, E. J., and Cobb, M. H. (1994) *Curr. Opin. Struct. Biol. 4*, 833−40.
59. Prowse, C. N., Hagopian, J. C., Cobb, M. H., Ahn, N. G., and Lew, J. (2000) *Biochemistry 39*, 6258−66.
60. Albery, W. J., and Knowles, J. R. (1976) *Biochemistry 15*, 5631−40.
61. Albery, W. J., and Knowles, J. R. (1977) *Angew Chem. Int. Ed. Engl. 16*, 285−93.
62. Schowen, K. B., and Schowen, R. L. (1982) *Methods Enzymol. 87*, 551−606.

BI010959E